Russian Journal of Earth Sciences

Reproducing the Variability of the Thermal State of Lake Ladoga in 1980–2020 Based on Two Models of Thermohydrodynamics

V. A. Ryabchenko*[,1], A. V. Isaev[1], A. A. Konik[1], S. D. Golosov[1,2], and I. S. Zverev[1,2]

[1] Shirshov Institute of Oceanology, Russian Academy of Sciences, Moscow, Russian Federation
[2] Institute of Limnology, Saint Petersburg Federal Research Center, Russian Academy of Sciences, Saint-Petersburg, Russian Federation
* **Correspondence to:** V.A. Ryabchenko, vla-ryabchenko@yandex.ru

Abstract: The results of reproducing the thermal state of Lake Ladoga in the period 1980–2020 using two models, the St. Petersburg Baltic Eutrophication Model (SPBEM) of the St. Petersburg Branch of the Shirshov Institute of Oceanology of the RAS, and the Inland Sea Hydrodynamics Model (ISHM) of the Institute of Limnology of the RAS, are compared with available data from contact and satellite measurements, as well as with each other. In general, both models adequately reproduce the main features of the average state and intra-annual variability of the lake. The long-term annual averages of the surface temperature of Lake Ladoga based on the MODIS Aqua (2002–2020), MODIS Terra (2000–2020) and Suomi NPP VIIRS (2012–2020) data are 7.75, 7.66 and 7.90 °C, respectively, while the SPBEM estimates are underestimated by 1.00, 0.96 and 1.00 °C, respectively, and the ISHM estimates are underestimated by 0.66, 0.57 and 0.54 °C. The interannual trends in the surface temperature calculated using satellite data were statistically insignificant at a 95% confidence level. The average annual modeled surface temperature in the period 1980–2020, according to statistically significant linear trends, increased by 1.2 (1.7)°C, respectively, according to SPBEM and ISHM. The temperature increase was 1.6 (2.6)°C during the summer period and 0.8 (1.0)°C in the winter. The average annual temperature of the entire lake changed by 0.5 (0.8)°C. SPBEM and ISHM overestimate the observed average ice area of 7816 km^2 for the period 1980–2020 by 15 and 14%, respectively; its annual averages decreased by 85, 68 and 108 km^2 per year according to SPBEM, ISHM and observations.

Keywords: Intra-annual and interannual variability, temperature, ice, modeling, satellite and in situ observations, Lake Ladoga

Citation: Ryabchenko V. A., Isaev A. V., Konik A. A., Golosov S. D., and Zverev I. S. (2026), Reproducing the Variability of the Thermal State of Lake Ladoga in 1980–2020 Based on Two Models of Thermohydrodynamics, *Russian Journal of Earth Sciences*, 26, ES1010, EDN: DMJUXH, https://doi.org/10.2205/2026es001058

Research Article

Received: March 18, 2025
Accepted: September 8, 2025
Published: March 27, 2026

1. Introduction

The current state of Lake Ladoga is described based on contact and satellite observations in a recent monograph [*Current state...*, 2021]. Processing the archive of available observation data made it possible to identify the main large-scale features of seasonal and interannual variability of hydrophysical, hydrochemical and hydrobiological indicators. However, a complete picture of this variability for all main physical and biogeochemical characteristics can only be reconstructed based on model calculations.

A characteristic feature of large stratified inland water bodies, which include Lake Ladoga, is the fact that their horizontal size is much larger than the baroclinic Rossby radius of deformation. Therefore, models developed for oceans and seas are used to model such water bodies. Currently, widespread modern model complexes used in the ocean (MITgcm, NEMO, Delft 3D and others), as well as specialized 1-D and 2-D models developed for

lakes are used to reproduce the hydrothermodynamics of large stratified inland water bodies. The use of oceanic hydrothermodynamic models in freshwater lakes is preceded by their adaptation to lake conditions, including the exclusion of salinity from the model variables, a corresponding change in the equation of state, and the introduction of freshwater ice. A detailed review of the models used to reproduce the hydrothermodynamics and ecosystems of inland water bodies is presented in [*Ménesguen and Lacroix*, 2018; *Mooij et al.*, 2010; *Vinçon-Leite and Casenave*, 2019].

Since the 1980s, several original eco-hydrodynamic models of the Lake Ladoga ecosystem have been developed [*Ladoga...*, 2010; *Menshutkin et al.*, 1998; *Rukhovets et al.*, 2003]. The use of these models made it possible to assess the response of the Lake Ladoga ecosystem to an increase in phosphorus load and to identify maximum permissible loads. However, these models were implemented on coarse computational grids, and the runs with them were performed to reach a periodic climatic solution under fixed external forcing, which did not allow reproducing the long-term variability of ecosystem characteristics [*Current state...*, 2021].

This study uses two hydrothermodynamic models that are free from these disadvantages. The first model is based on one of the advanced general circulation models MITgcm [*Marshall et al.*, 1997], which has been successfully used to simulate not only the World Ocean but also the dynamics of the Great American Lakes [*Bennington et al.*, 2010; *Pilcher et al.*, 2015]. This model, called the St. Petersburg Baltic Eutrophication Model (SPBEM) [*Isaev et al.*, 2020; *Ryabchenko et al.*, 2016], was previously adapted to the conditions of Lake Ladoga [*Isaev and Savchuk*, 2020], but on a grid with a horizontal resolution of about 4 km, which did not allow, in particular, to reproduce the thermal bar, one of the most important physical characteristics for the functioning of the ecosystem of a freshwater reservoir. The first calculations of the lake hydrothermodynamics for the modern climatic period on a high-resolution grid (≈1 km) using this model were recently performed in [*Isaev et al.*, 2024]. The second model is a completely domestic development [*Ibrayev*, 2001], which was successfully used to model the Caspian Sea [*Ibrayev*, 2008]. This model, called the Internal Sea Hydrodynamic Model (ISHM), was used to reproduce thermohydrodynamic processes over water exchange time periods for Ladoga of 12–14 years [*Golosov et al.*, 2020; *Zverev et al.*, 2020]. The choice of these two models for this study is due to their successful application for Ladoga and other large inland water bodies in previous studies.

This paper reproduces the variability of the thermal state of Lake Ladoga in 1980–2020 based on two high-resolution thermohydrodynamic models. The use of two models increases the reliability of the results of model calculations, which are compared with all available observations to establish the adequacy of the developed models. In addition, the model results complement the picture of the features of the seasonal and interannual variability of Lake Ladoga in the time and space intervals of the absence of observations. The quality of reproduction of the thermal regime, one of the main factors determining the state of the lake ecosystem, plays a key role in adequately reproducing the variability of the lake ecosystem, which is the target of this work in the future.

2. Methods and Data

Brief description of the models. The calculations of the thermohydrodynamics of Lake Ladoga were performed based on the above two thermohydrodynamic models: SPBEM and ISHM. The calculations covered the period from January 1, 1980 to December 31, 2020. The main parameters, parameterizations and external forcings in the two compared models are given in Table 1.

As seen, the models are implemented on the same grid with a 1-km horizontal resolution and a variable vertical resolution of 2–5 m, and use the same depth archive. The parameterizations of a number of physical processes (horizontal turbulence scheme for momentum, convection, short- and long-wave radiation on the lake surface) in the models are the same. However, the parameterizations of most physical processes (vertical turbulence and horizontal turbulence schemes for T and S, equation of state, wind friction

Table 1. Main parameters, parametrizations and external forcings in the two compared models

Model ID	SPBEM (St. Petersburg Baltic Sea Eutrophication Model)	ISHM (Inland Sea Hydrodynamics Model)
Depth field	Data from the Institute of Limnology of the RAS	Data from the Institute of Limnology of the RAS
Horizontal grid	Spherical Arakawa *C* grid with using *D* grid for Coriolis terms calculation on next time step [*Marshall et al.*, 1997]	Spherical Arakawa *C* grid [*Marshall et al.*, 1997]
Horizontal resolution	$\Delta\varphi = 0.54'$, $\Delta\lambda = 1.08'$ (≈ 1 km × 1 km)	$\Delta\varphi = 0.54'$, $\Delta\lambda = 1.08'$ (≈ 1 km × 1 km)
Vertical grid	*Z*-coordinate	*Z*-coordinate
Vertical resolution	$\Delta z = 2$ m at $0\,\text{m} \le z < 40$ m $\Delta z = 5$ m at $40\,\text{m} \le z < H$	$\Delta z = 2$ m at $0\,\text{m} \le z < 40$ m $\Delta z = 5$ m at $40\,\text{m} \le z < H$
Vertical turbulence scheme[1]	TKE closure scheme [*Gaspar et al.*, 1990]	Munk–Anderson scheme [*Munk and Anderson*, 1948]
Horizontal turbulence scheme for momentum[2]	*Smagorinsky et al.* [1965]	*Smagorinsky et al.* [1965]
Horizontal turbulence scheme for *T* and *S*	$KT = \text{const} = 2\,\text{m}^2/\text{s}$	$KT = \text{const} = 5\,\text{m}^2/\text{s}$
Solution method	Preconditioned conjugate-gradient solution method for 2D and 3D elliptic problems for the pressure [sections 4.1.1 and 4.1.2 in *Marshall et al.*, 1997]	The solution of the equations is divided into the solution of the 3D equations for baroclinic motions and the solution of the 2D shallow water equations for barotropic motions [*Ibrayev*, 2001]
Convection	Hydrostatic model, convection is parameterized through enhanced vertical diffusion with $Kz = 100\,\text{m}^2/\text{s}$ [*Klinger et al.*, 1996]	Hydrostatic model, convection is parameterized through varying vertical diffusion
Equation of state	[*TEOS-10*, 2010]	[*Chen and Millero*, 1986]
Wind stress	[*Large and Pond*, 1981]	[*Launiainen and Vihma*, 1990]
Sea surface heat fluxes:		
1. Short-wave radiation	From [*Hersbach et al.*, 2023]	From [*Hersbach et al.*, 2023]
2. Long-wave radiation:		
a) incoming	From [*Hersbach et al.*, 2023] Stefan-Boltzmann law	From [*Hersbach et al.*, 2023] Stefan-Boltzmann law
b) outgoing	From [*Hersbach et al.*, 2023] Stefan-Boltzmann law	From [*Hersbach et al.*, 2023] Stefan-Boltzmann law
3. Sensible heat flux	[*Large and Pond*, 1981]	[*Launiainen and Vihma*, 1990]
4. Latent heat flux	[*Large and Pond*, 1981]	[*Launiainen and Vihma*, 1990]
Bottom friction	no-slip condition	Quadratic friction, accounting for the rotation of the velocity vector in the bottom layer [*Ibrayev and Trukhchev*, 1998]
Ice model	`SeaIce` package of the `MITgcm`, adapted for a freshwater reservoir [*Hibler*, 1980; *Zhang and Hibler*, 1997], accounting for ice dynamics	Hibler sea ice model [*Hibler*, 1980], no ice drift
Rivers	Prescribed volume transport [*Isaev et al.*, 2024] Zero heat and salt fluxes	Prescribed volume transport [*Isaev et al.*, 2024] Prescribed heat and salt fluxes from inflowing rivers

Notes: [1] The SPBEM model uses a turbulent scheme [*Gaspar et al.*, 1990], in which one differential equation for the TKE k is solved. The coefficients of turbulent viscosity K_m and diffusion K_h are calculated using the formulas: $K_m = c_k l\sqrt{k}$, $K_h = c'_k l\sqrt{k}$, where $l = \sqrt{2k}/N$ – is the mixing scale, $N = \left(-g\rho_0^{-1}\rho_z\right)^{1/2}$ is the Brunt–Väisälä frequency, g is the gravitational acceleration, ρ and ρ_0 are the density and its reference value, c_k *and* c'_k are the stability functions. In [*Gaspar et al.*, 1990], it is assumed that $c_k = 0.1$, $c'_k = \frac{c_k}{P_{rt}}$, where the turbulent Prandtl number $P_{rt}$is taken to be equal to 1. The ISHM model implements a simpler approach. The coefficients K_m and K_h are calculated through the Richardson number Ri using the formulas: $K_m = \frac{K_{m0}}{(1+aRi)^b}$, $K_h = \frac{K_{h0}}{(1+a'Ri)^{b'}}$, where K_{m0} and K_{h0} are the background values of K_m and K_h, a, b, a', b' are empirical constants, $Ri = \frac{g\rho_0^{-1}\rho_z}{\left[(U_z)^2+(V_z)^2\right]}$, (U, V) are the horizontal velocity components [*Munk and Anderson*, 1948].

[2] Smagorinsky's formula for the subgrid coefficient of horizontal turbulent viscosity K_V can be represented as (in Cartesian coordinates): $K_V = ch_xh_yS$, $S = \left(2\,S_{ij}S_{ji}\right)^{1/2}$, $S_{ij} = \frac{1}{2}\left(\partial_i U_j + \partial_j U_i\right)$, where $c = 0.2$ is a constant; h_x and h_y are the grid steps in x and y directions; U_i $(i = 1, 2)$ are the components of the horizontal velocity.

stress, surface sensible and latent heat fluxes, bottom friction, conditions at the boundaries with rivers) in the models, as well as the method for solving the system of equations, differ from each other. The most significant differences are different parameterizations of vertical mixing in the models and the allowance for ice drift in SPBEM and the absence of ice drift in ISHM.

Initial conditions. Since the data of field observations are insufficient to form consistent fields of thermohydrodynamic variables, then to obtain the initial distribution of the model variables, a run was performed with repeating boundary conditions (atmospheric forcing and river runoff specified as indicated in Table 1) corresponding to the conditions of 1979, until a quasi-steady-state of the intra-annual variability of the lake was obtained. The values of the sought physical characteristics on January 1, 1979 in this quasi-steady-state were used as initial conditions for calculating the state of Lake Ladoga in the period 1979–2020. The calculation for 1979 during the model run for the specified long period was attributed to the model acceleration stage and was not taken into account in the analysis.

Observational data. To verify the temperature characteristics of the SPBEM and the ISHM, 4818 fields (see Table 2) of the surface temperature of Lake Ladoga from January to December 2000–2020 were used, obtained from the MODIS Aqua (2002–2020), MODIS Terra (2000–2020), Suomi NPP VIIRS (2012–2020) satellites of the L2 processing level (includes the measurement time, georeferencing and processing of the original signal taking into account the atmospheric correction). Of all the available data marked with 5 quality quartiles (SST_{qual}): 0 (excellent), 1 (good), 2 (average), 3 (poor), 4 (raw), only the data of the first three quartiles – 0, 1 and 2 – were used to construct the surface temperature maps. In addition, only satellite fields covering at least 20% of the lake area were used. To verify the vertical structure of the waters of Lake Ladoga, contact temperature measurement data obtained by employees of the Institute of Limnology of the Russian Academy of Sciences (RAS) in the period 1991–2013 were used. The calculated ice area was compared with its estimates from [*Current state...*, 2021].

Table 2. Number of high-quality satellite images ($SST_{qual} = 0, 1, 2$) [*NASA*, 2024] used to calculate monthly average statistical characteristics of Lake Ladoga surface temperature

Satellite/month	MODIS Aqua	MODIS Terra	SUOMI NPP VIIRS
January	13	23	11
February	15	11	7
March	46	52	29
April	144	169	104
May	265	291	266
June	186	193	273
July	304	355	297
August	276	281	274
September	170	177	174
October	88	82	64
November	33	41	36
December	27	22	19

Comparison procedure. The procedure for comparing the surface temperature reproduced by the SPBEM and ISHM models with satellite data consisted of several steps. At the first step, instantaneous satellite temperature fields were interpolated onto the model grid. Surface temperature fields corresponding to the observation dates were selected from the modeling results, while only areas with satellite measurement data were considered for comparison; in areas with no measurement data (due to cloudiness or ice), model data were not considered, i.e. they were assumed to be missing. The following statistical characteristics were calculated from the time- and space-matched surface temperature fields of Lake Ladoga: the mean (over the lake surface) value $\langle T \rangle$, standard deviation σ,

correlation coefficient R between each of the models and each of the satellites and the significance level p_{level} for differences between average values of satellite and model data. Based on the statistical characteristics calculated for the instantaneous fields, their average monthly values were calculated and are presented in Table 3.

Average long-term state of the entire Lake Ladoga in the warm part of the year. In order to understand how well the models reproduce the climatic state of Lake Ladoga, the average lake temperatures for the warm part of the year (May–September) were calculated for the period 1991–2013. Only the warm part of the year was considered due to fragmentation and a small number of observational data in the autumn-winter period. According to the observational data, the temperature averaged over the warm part of the year for the entire Lake Ladoga in the specified period was 6.46 °C with a minimum of 4.58 °C (25% quantile) and a maximum of 7.96 °C (75% quantile). Estimates using the SPBEM and ISHM models gave average temperature values of 6.0 and 6.4 °C, minimums of 5.85 and 6.13 °C, and maximums of 6.18 and 6.61 °C, respectively. Thus, the model estimates of the average temperature of Lake Ladoga during the warm part of the year turned out to be somewhat underestimated compared to observational data.

To compare the model and actual estimates of *the average annual long-term state of Lake Ladoga*, estimates based on the database of temperature measurements in Lake Ladoga [*Naumenko and Guzivaty*, 2010] were used, according to which the average annual temperature of the entire Lake Ladoga for the period 1898–2010 was 3.8 °C with a minimum of 3.3 °C (25% quantile) and a maximum of 4.4 °C (75% quantile). This climatic period includes the cooling period of 1940–1970 in the Northern Hemisphere, which should be taken into account when comparing with similar estimates based on models related to the period 1980–2010. Similar average annual values, their minimum and maximum estimates of lake temperature for the period 1980–2010. according to the SPBEM model are 4.29, 4.18 and 4.42 °C, respectively, and according to the ISHM model – 4.82, 4.62 and 4.98 °C. Considering the discrepancy between the averaging periods of natural and model data, as well as the proximity of the SPBEM model estimates to the estimate of the maximum temperature (75% quantile) according to observational data, it can be concluded that the SPBEM model satisfactorily reproduces the climatic average annual temperature of the lake. At the same time, the ISHM model somewhat overestimates it.

Average state and intra-annual variability. As follows from Table 3, the long-term average annual values of the surface temperature of Lake Ladoga according to the MODIS Aqua, MODIS Terra and Suomi NPP VIIRS satellites are 7.75, 7.66 and 7.90 °C, respectively, while the estimates from the SPBEM are underestimated by 1.00, 0 · 96 and 1.00 °C, respectively, and the estimates from the ISHM are underestimated by 0.66, 0.57 and 0.54 °C. As can be seen from Table 3 and Figure 1, during the annual cycle, the difference ΔT between the monthly average values of the satellite $\langle \overline{T} \rangle_{\text{sat}}$ and the model $\langle \overline{T} \rangle_m$ surface temperature of Lake Ladoga was positive in all cases for SPBEM and in most cases for ISHM (except for June for all three satellites, May in the case of Suomi NPP VIIRS, October, November and December in the case of MODIS Terra, and November in the case of MODIS Aqua, when ΔT was negative, at most slightly exceeding 1 °C). The maximum values of ΔT were reached in July, when it was ΔT = 2.57, 2.36 and 1.76°C for the difference in estimates, respectively, from MODIS Aqua, MODIS Terra and Suomi NPP VIIRS data and the SPBEM, and ΔT = 2.37, 2.12 and 1.20 °C for the difference in the same satellite estimates and estimates from the ISHM. This underestimation of the lake surface temperature in summer is due to the fact that satellites measure the temperature of the surface itself, while the model data represent the average value for the upper two-meter layer. Therefore, given that in July – the first half of August the weakest winds and vertical mixing are observed, contributing to the formation of a vertical temperature gradient near the lake surface, the indicated underestimation of the surface temperature by the models is quite acceptable. With the onset of autumn and the beginning of intensive wind-wave and convective mixing, the absolute values of ΔT noticeably decrease and reach a minimum of 0.21 °C (November), 0.21 °C (November) and 0.34 °C (October) for the difference between satellite estimates and

Table 3. Monthly average statistical characteristics of the area-averaged surface temperature of Lake Ladoga based on data from the SPBEM and ISHM and the MODIS Aqua (2002–2020), MODIS Terra (2000–2020), and Suomi NPP VIIRS (2012–2020) satellites: $\langle\overline{T}\rangle_{\text{sat}}$ – mean value of satellite temperature measurements; $\langle\overline{T}\rangle$ SPBEM – mean temperature value in the SPBEM; $\langle\overline{T}\rangle$ $ISHM$ – mean temperature value in the ISHM; $\overline{\sigma}_{\text{sat}}$ – standard deviation of satellite temperature measurements; $\overline{\sigma}$ SPBEM – standard deviation of temperature in the SPBEM; $\overline{\sigma}$ ISHM – standard deviation of temperature in the ISHM; $\overline{R}$ SPBEM – correlation between satellite data and SPBEM model data; $\overline{R}$ ISHM – correlation between satellite data and ISHM model data; $\overline{p}_{\text{level}}$ SPBEM – significance level of the difference between $\langle\overline{T}\rangle_{\text{sat}}$ and $\langle\overline{T}\rangle$ SPBEM; $\overline{p}_{\text{level}}$ ISHM – significance level of the difference between $\langle\overline{T}\rangle_{\text{sat}}$ and $\langle\overline{T}\rangle$ ISHM; the overbar indicates monthly averaging, angle brackets indicate averaging over the lake surface.

Satellite	Month	$\langle\overline{T}\rangle_{\text{sat}}$	$\langle\overline{T}\rangle$ SPBEM	$\langle\overline{T}\rangle$ ISHM	$\overline{\sigma}_{\text{sat}}$	$\overline{\sigma}$ SPBEM	$\overline{\sigma}$ ISHM	$\overline{R}$ SPBEM	$\overline{R}$ ISHM	$\overline{p}_{\text{level}}$ SPBEM	$\overline{p}_{\text{level}}$ ISHM
MODIS Aqua	1	2.68	1.93	1.76	0.64	0.78	1.18	0.72	0.54	0.18	0.01
	2	1.09	0.32	0.21	0.52	0.25	0.27	0.35	0.07	0.11	0.01
	3	1.03	0.19	0.36	0.34	0.18	0.35	0.32	0.19	0.06	0.01
	4	1.75	0.81	1.31	0.61	0.53	0.56	0.49	0.09	0.07	0.01
	5	4.12	3.32	4.05	1.81	1.54	1.51	0.85	0.57	0.26	0.01
	6	11.20	9.91	11.46	2.70	2.58	2.77	0.83	0.68	0.17	0.96
	7	18.71	16.14	16.34	1.32	1.49	3.44	0.58	0.49	0.06	0.01
	8	18.48	16.38	16.69	0.86	1.23	3.42	0.51	0.40	0.06	0.01
	9	14.21	13.17	13.45	0.74	1.17	2.94	0.57	0.42	0.06	0.01
	10	9.32	9.07	9.18	0.70	0.98	2.10	0.59	0.50	0.46	0.92
	11	6.36	6.15	6.50	0.70	0.82	1.62	0.73	0.67	0.61	0.96
	12	4.02	3.55	3.83	0.74	0.86	1.36	0.82	0.86	0.29	0.69
MODIS Terra	1	2.29	1.57	1.34	0.75	0.77	1.04	0.71	0.45	0.09	0.05
	2	1.35	0.56	0.35	0.46	0.35	0.43	0.40	0.25	0.24	0.13
	3	1.06	0.15	0.40	0.37	0.17	0.41	0.28	0.15	0.06	0.01
	4	1.83	0.83	1.32	0.64	0.54	0.59	0.50	0.03	0.06	0.02
	5	4.03	3.32	4.03	1.79	1.51	1.48	0.85	0.58	0.14	1.00
	6	10.96	9.72	12.22	2.87	2.70	2.71	0.85	0.63	0.17	0.05
	7	18.59	16.23	16.47	1.32	1.50	3.40	0.62	0.54	0.05	0.01
	8	18.28	16.37	16.72	0.88	1.29	3.50	0.56	0.49	0.06	0.01
	9	13.99	13.08	13.11	0.74	1.24	2.80	0.58	0.45	0.03	0.17
	10	9.33	9.09	9.54	0.70	0.99	2.11	0.54	0.42	0.66	0.78
	11	6.27	6.06	6.71	0.72	0.83	1.51	0.71	0.55	0.44	0.90
	12	3.91	3.39	4.07	0.84	0.93	1.42	0.83	0.82	0.22	0.49
Suomi NPP VIIRS	1	2.86	1.93	1.27	0.42	0.57	0.87	0.67	0.47	0.15	0.01
	2	1.67	0.54	0.29	0.29	0.25	0.32	0.36	0.15	0.06	0.03
	3	1.37	0.27	0.35	0.33	0.21	0.38	0.42	0.32	0.05	0.01
	4	2.08	1.01	1.73	0.67	0.54	0.56	0.49	0.10	0.05	0.16
	5	4.43	3.57	4.88	1.85	1.52	1.57	0.88	0.73	0.08	0.44
	6	11.54	10.31	12.58	2.56	2.42	2.37	0.82	0.65	0.49	0.60
	7	17.50	15.74	16.30	1.15	1.22	2.84	0.57	0.49	0.05	0.02
	8	17.79	16.14	16.62	0.83	1.01	3.06	0.56	0.53	0.05	0.08
	9	14.49	13.54	13.87	0.64	0.92	2.59	0.52	0.38	0.14	0.03
	10	9.42	9.08	9.36	0.70	0.84	1.70	0.57	0.52	0.34	0.80
	11	6.69	6.32	6.55	0.57	0.68	1.44	0.65	0.57	0.26	0.62
	12	4.98	4.31	4.56	0.56	0.65	1.20	0.78	0.75	0.24	0.70

Note: The insignificance level p_{level} of the difference between the average (over the lake surface) values of satellite and model data was estimated using the formulas:

$$t = \Big(\langle x\rangle_1 - \langle x\rangle_2\Big)\Big/\sqrt{\frac{\sigma_1^2}{n_1 + \frac{\sigma_2^2}{n_2}}}, \quad p_{\text{level}} = 2\Big(1 - F_t(|t|, df)\Big),$$

where $\langle x\rangle_1$ and $\langle x\rangle_2$ are the mean values of the series (samples) of satellite and model data, σ_1 and σ_2 are the standard deviations of the samples, n_1 and n_2 are the sample sizes, $df = n_1 + n_2 - 2$ is the number of degrees of freedom, F_t is the Student's distribution function. At $p_{\text{level}} \geq 0.05$, the difference between the series is statistically insignificant.

the SPBEM, and 0.14 °C (October), 0.16 °C (December) and 0.06 °C (October) for a similar difference between satellite estimates and the ISHM. According to the estimates of the significance level $\overline{p}_{\text{level}}$, the difference between the average monthly values of satellite $\langle\overline{T}\rangle_{\text{sat}}$ and $\langle\overline{T}\,\rangle$ SPBEM data is insignificant for all months of the year and all satellites used, while a similar difference in the case of the ISHM is significant for different satellites both in the warm period of the year (May, June, July) and in the cold period (October, November, December, March).

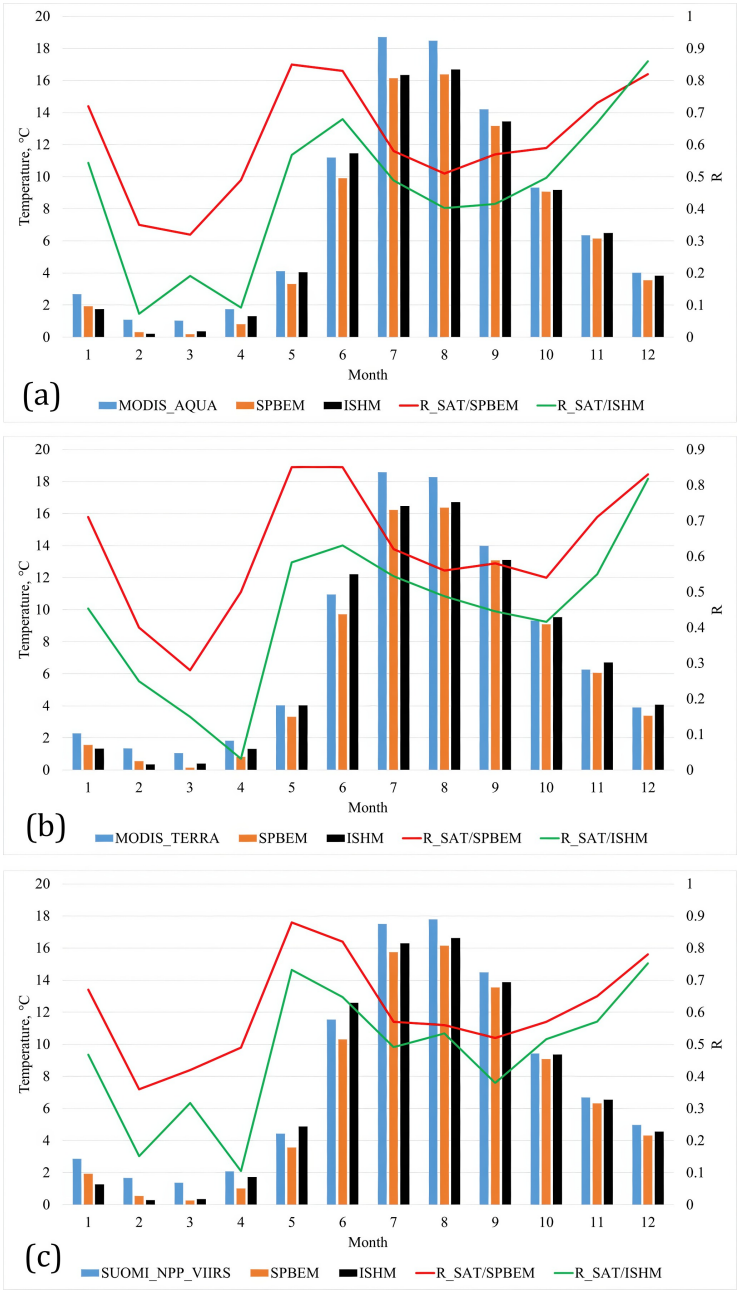

Figure 1. Intra-annual variability of the surface temperature of Lake Ladoga and the correlation coefficients between satellite measurements and model calculations: a – results of Aqua MODIS measurements and SPBEM and ISHM calculations; b – results of Terra MODIS measurements and SPBEM and ISHM calculations; c – results of SUOMI NPP VIIRS measurements and SPBEM and ISHM calculations. In all figures, blue columns show satellite measurements, orange – SPBEM data, black – ISHM data, the red curve is the correlation coefficient between satellite measurements and the SPBEM, the green curve is the correlation coefficient between satellite measurements and the ISHM.

Assessing the quality of the models under consideration in relation to reproducing the average surface temperature of Lake Ladoga, we note that although SPBEM slightly (on average by no more than 0.4 °C) underestimates the temperature estimated from satellite data than ISHM, it generally reproduces the standard deviation of this characteristic better (Table 3), has insignificant deviations of monthly average values from satellite data and correlates better with them, especially during the ice cover period (Figure 1).

The quality of reproduction of the spatial distribution of the surface temperature of Lake Ladoga can be assessed by Figure 2, which shows the average long-term (for the period 2000–2020) monthly fields of the surface temperature of Lake Ladoga in May and June (the period of existence of the thermal bar), obtained from the averaged data of three satellites and the results of calculations for each of the models. As can be seen, the SPBEM model distributions correspond better to the satellite images: the temperature gradient in the southeast-northwest direction is more pronounced, the position of the 4 °C isotherm in May is reproduced almost exactly.

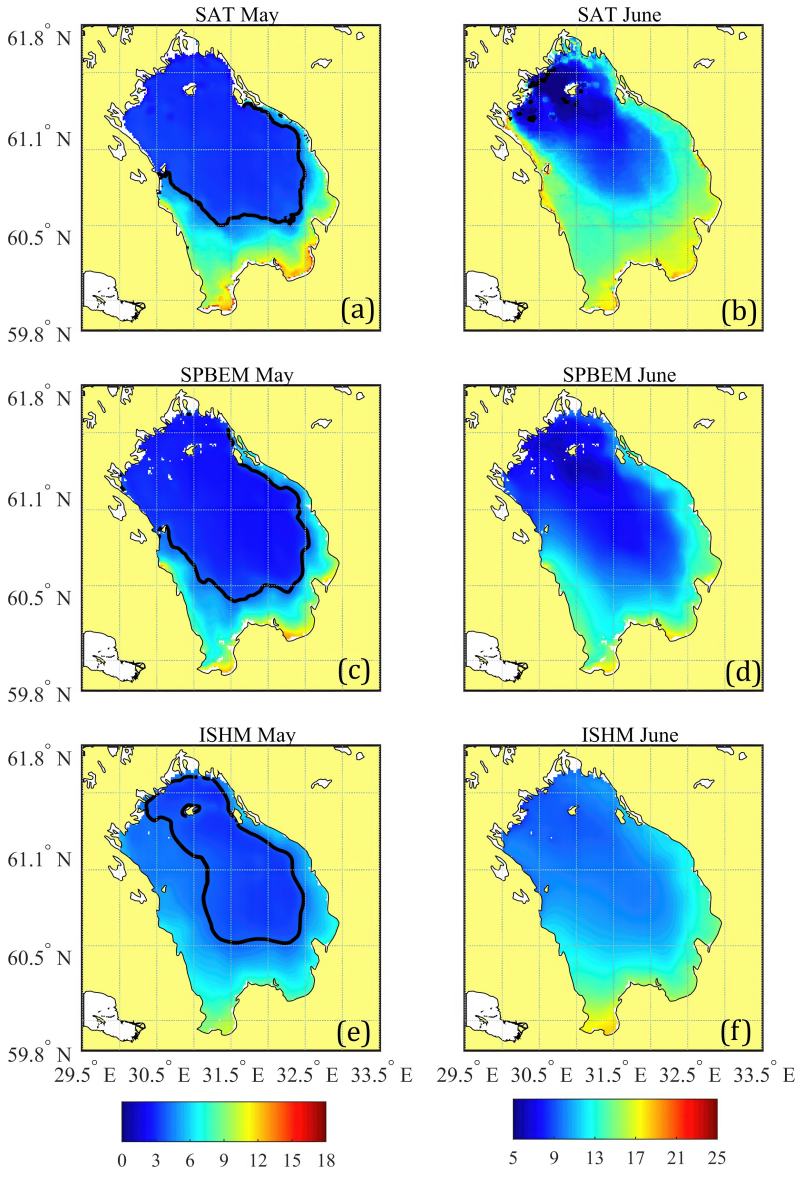

Figure 2. Average long-term (for the period 2000–2020) distributions of surface temperature (°C) of Lake Ladoga for May (a, c, e) and June (b, d, f) based on averaged satellite data from Aqua MODIS, Terra MODIS and SUOMI NPP VIIRS (a, b) and results from SPBEM (c, d) and ISHM (e, f). The black line shows the position of the 4 °C isotherm.

The average vertical distributions of the monthly mean temperature in the central deep-water part of Lake Ladoga for the period 1991–2013, obtained from expeditionary measurements and SPBEM and ISHM results are shown in Figure 3. As seen, both models accurately reproduce the temperature at depths greater than 80 m for the entire period under consideration (May–September). The temperature in the overlying layers is reproduced with high accuracy by the SPBEM model. The ISHM model significantly overestimates the observed temperature in the (0–50 m) layer in May, in the (0–20 m) layer in June, and in the (20–50 m) and (20–80 m) layers in August and September, respectively. This overestimation is apparently related to the poorly adapted to lake conditions parameterization of vertical mixing in terms of the Richardson number [*Munk and Anderson*, 1948], which is rarely used in modern three-dimensional numerical models of ocean circulation.

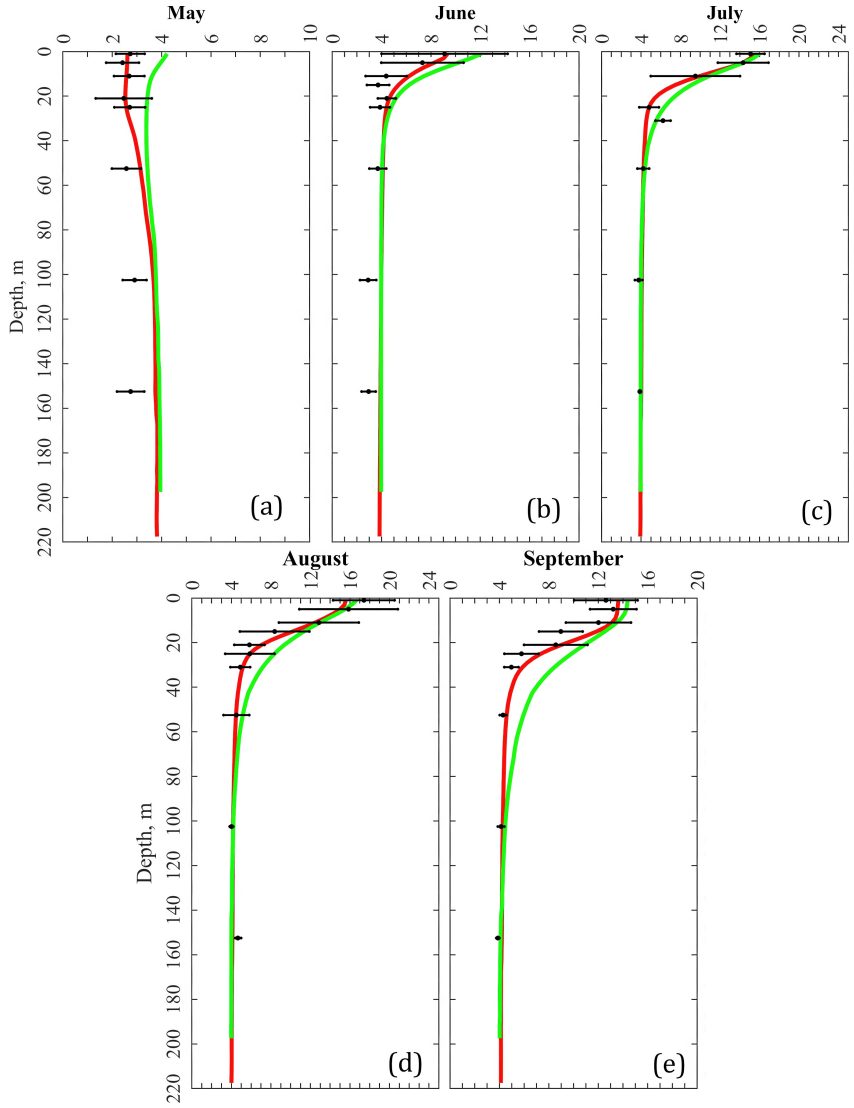

Figure 3. Average vertical temperature distributions (°C) for the period 1991–2013, averaged over the central deep-water part of Lake Ladoga, in May (a), June (b), July (c), August (d), and September (e) based on expeditionary measurements (dots are average values, black horizontal lines are standard deviations) and the results of the SPBEM (red curves) and the ISHM (green curves). The deep-water part of the lake is identified by the position of the 40-meter isobath.

Interannual variability. Figure 4 and Table 4 present the characteristics of the interannual variability of the mean summer (June–September) surface temperature of Lake Ladoga for the satellite measurement period of 2000–2020. As seen, the calculated mean temperatures and variances are underestimated compared to the satellite data, the trends

Table 4. Statistical characteristics of the temperature series shown in Figure 4: $\langle\overline{T}\rangle$ – average temperature, °C; $\overline{D}$ – variance, °C^2; b – trend coefficient, °C^{-1}; R^2 – determination coefficient; $\overline{p}_{\text{level}}$ – significance level; $\overline{R}$ – correlation coefficient of satellite and model data

Parameter	Data source				
	SAT	*SPBEMSAT*	*ISHMSAT*	*SPBEM*	*ISHM*
$\langle\overline{T}\rangle$	16.11	14.37	14.75	13.50	14.66
$\overline{D}$	2.75	1.46	1.53	0.46	0.61
b	−0.060	−0.043	−0.024	0.008	0.044
R^2	0.05	0.05	0.01	0.01	0.12
$\overline{p}_{\text{level}}$	0.33	0.33	0.61	0.75	0.12
$\overline{R}$	–	0.97	0.92	0.79	0.71

are contradictory: according to the satellite data and in the case of averaging the model data over the surface masked as a satellite, the trends in the specified period are negative, and in the case of averaging the model data over the entire surface of the lake, they are positive. But the most important thing is that all trends are statistically insignificant. Therefore, in order to obtain statistically significant estimates, we will not further consider short series of satellite data, relying only on long 40-year series of modeling results and ice observation data.

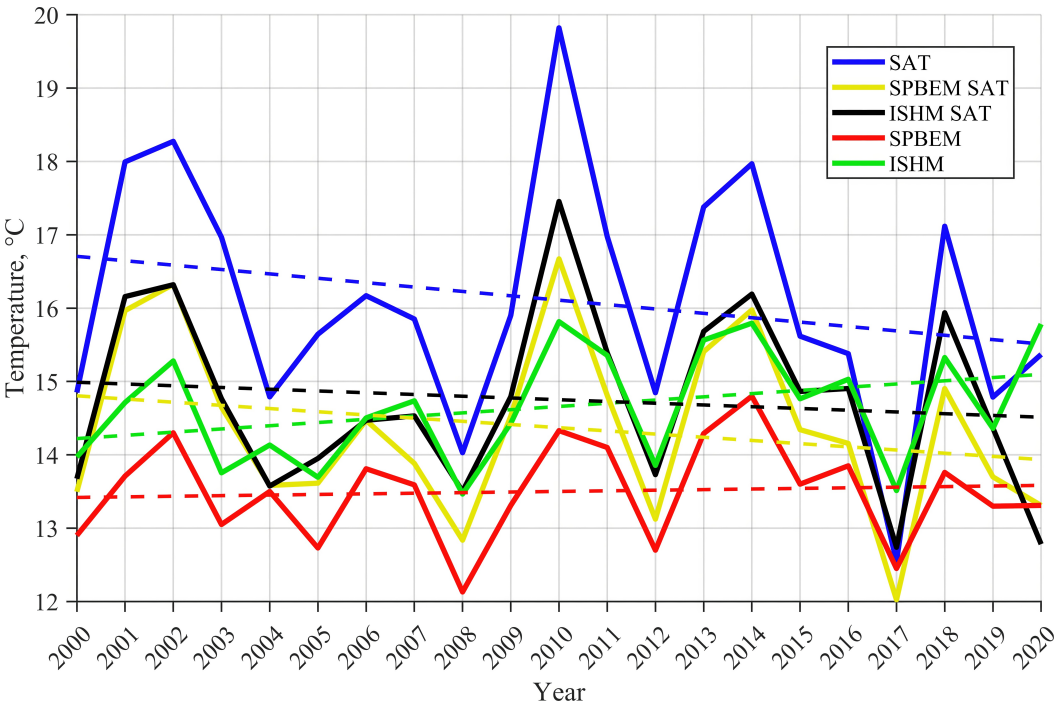

Figure 4. Interannual variability of the area-averaged mean summer (June–September) surface temperature of Lake Ladoga for the satellite measurement period 2000–2020: blue curve – averaged satellite (Aqua MODIS, Terra MODIS and Suomi NPP VIIRS) data (SAT); yellow curve – surface temperature masked as satellite in SPBEM; black curve – surface temperature masked as satellite in ISHM; red curve – surface temperature in SPBEM, green curve – surface temperature in ISHM.

3. Results and Discussion

According to the model data (see Figure 5 and Table 5), the area-averaged surface temperature of Lake Ladoga fluctuated in the period 1980–2020, with its mean annual value increasing (according to the trend) by 1.22 (1.68)°C from 5.43 (5.63)°C in 1980 to 6.65 (7.31)°C in 2020, respectively, in SPBEM and ISHM (Figure 5a). The temperature

increase was greater in the summer (June–September), when stable vertical stratification prevailed in the lake area, and it amounted to 1.64 (2.56)°C (Figure 5b), and less in the winter – 0.84 (0.96)°C (Figure 5c). At the same time, the mean annual temperature of the entire lake (from the surface to the bottom) in this period changed less than the surface temperature: from 4.10 (4.48)°C in 1980 to 4.62 (5.32)°C in 2020, respectively, according to SPBEM and ISHM, i.e. by only 0.52 (0.84)°C (Figure 5d).

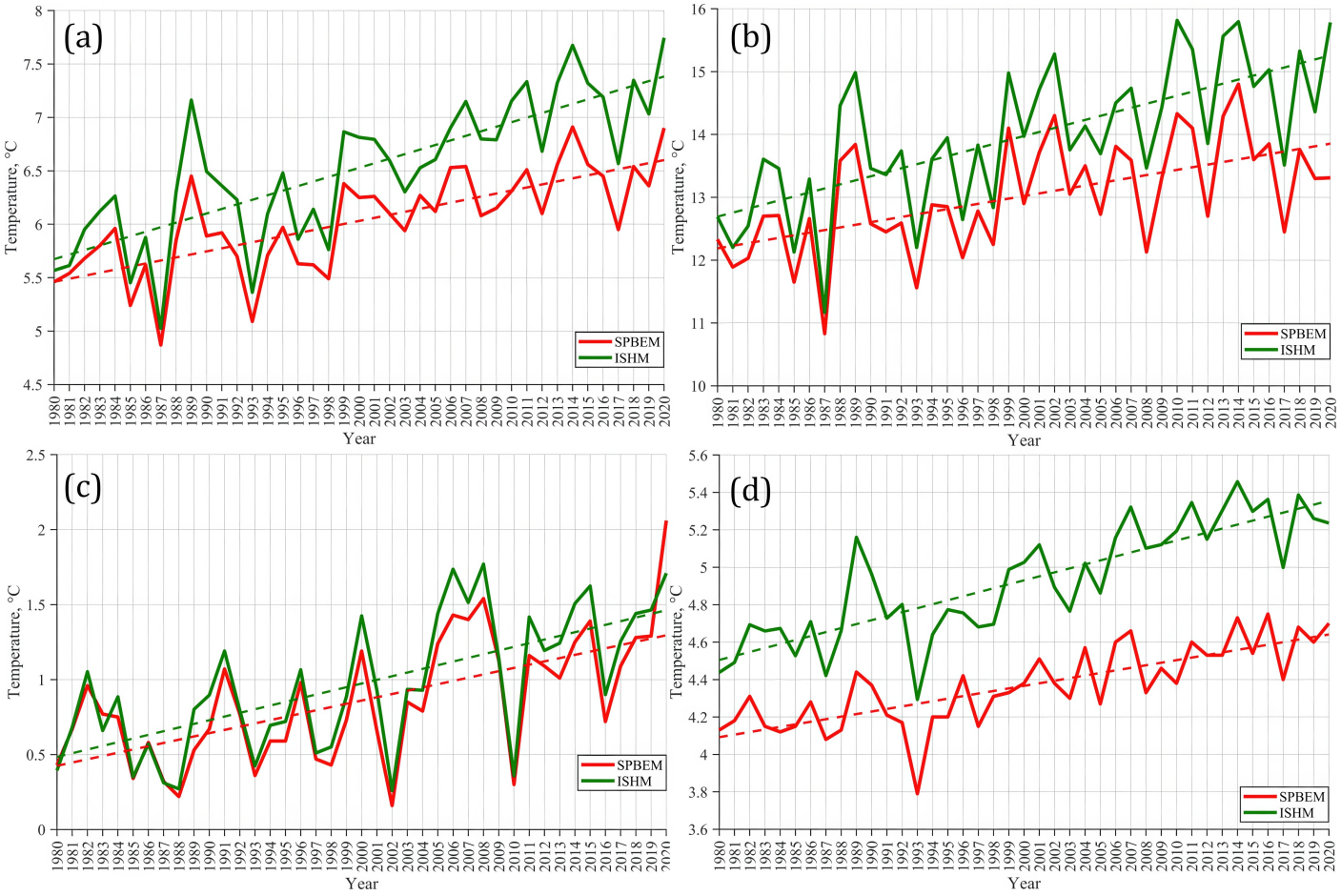

Figure 5. Interannual variability of the area-averaged surface temperature of Lake Ladoga according to SPBEM (red curves) and ISHM (green curves) for the period 1980–2020: a – mean annual surface temperature; b – mean summer (June–September) surface temperature; c – mean winter (December–February) surface temperature; d – mean annual temperature of the entire lake (from surface to bottom). Linear trends of characteristics are shown by dashed lines.

Table 5. Statistical characteristics of the temperature series shown in Figure 4: $\langle\overline{T}\rangle$ – average temperature, °C; $\overline{D}$ – variance, °C^2; b – trend coefficient, °C · year^{-1}; R^2 – determination coefficient; $\overline{p}_{\text{level}}$ – significance level; $\overline{R}$ – correlation coefficient of satellite and model data

Parameter	$\langle\overline{T}\rangle$		$\overline{D}$		b		R^2		$\overline{p}_{\text{level}}$		$\overline{R}$
Model	SPBEM	ISHM	SPBEM	ISHM	SPBEM	ISHM	SPBEM	ISHM	SPBEM	ISHM	
Figure 5a	6.03	6.53	0.22	0.42	0.028	0.043	0.54	0.62	5×10^{-8}	1×10^{-9}	0.98
Figure 5b	13.02	13.98	0.76	1.26	0.042	0.064	0.33	0.47	9×10^{-5}	8×10^{-7}	0.95
Figure 5c	0.86	0.97	0.17	0.2	0.022	0.024	0.39	0.43	1×10^{-5}	3×10^{-6}	0.96
Figure 5d	4.37	4.93	0.05	0.09	0.014	0.021	0.60	0.69	3×10^{-9}	2×10^{-11}	0.92

The duration of the spring thermal bar, determined by its onset and end dates, can serve as an indicator of interannual changes in the temperature field. As preliminary

calculations have shown, it is impossible to obtain reliable estimates of the onset and end dates of the thermal bar using satellite data, since these estimates can only be obtained using high-quality satellite images, which are quite rare, and the thermal bar could actually form in the interval between the dates of obtaining these images. Therefore, these satellite estimates were excluded from consideration, and Figures 6a and 6b and the relevant Table 6 present only the results of model estimates. Judging by the linear trends during the period under consideration, there was a shift in the onset of the thermal bar existence period by 115 – 107 = 8 (134 – 113 = 21) days towards the beginning of the year, and its duration slightly decreased from 179 – 115 = 64 (174 – 134 = 40) days in 1980 to 167 – 107 = 60 (152 – 113 = 39) days in 2020, respectively, according to SPBEM and ISHM. According to earlier studies [*Current state...*, 2021], the disappearance of the thermal bar in Lake Ladoga occurred in the first ten days of July, while according to the estimates presented above, a shift in the end time of the thermal bar is observed to the second ten days of June, which is a clear indicator of the impact of climate change on the hydrodynamic regime of the lake [*Groisman et al.*, 2017].

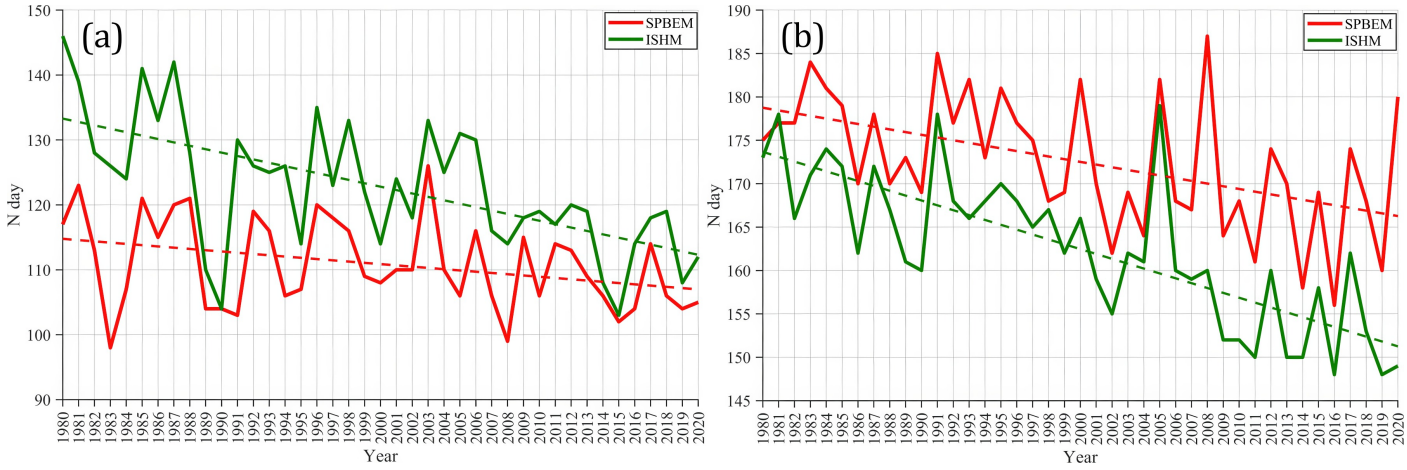

Figure 6. Day numbers of the onset and end of the thermal bar according to SPBEM (red curves) and ISHM (green curves): a – day number of the thermal bar onset; b – day number of the thermal bar end. Linear trends of the characteristics are shown by dashed lines.

Table 6. Statistical characteristics of the series of day numbers of the onset and end of the thermal bar, shown in Figure 6: $\overline{N_{day}}$ – average day number; D – variance; b – trend coefficient, year^{-1}; R^2 – determination coefficient; p_{level} – significance level; R – correlation coefficient between SPBEM and ISHM data.

Parameter	$\overline{N_{day}}$		D		b		R^2		$\overline{p}_{\text{level}}$		$\overline{R}$
Model	SPBEM	ISHM	SPBEM	ISHM	SPBEM	ISHM	SPBEM	ISHM	SPBEM	ISHM	
Figure 6a	111	123	48	105	–0.19	–0.52	0.11	0.38	0.03	2.0×10^{-5}	0.68
Figure 6b	173	162	59	75	–0.31	–0.56	0.24	0.60	0.001	2.5×10^{-9}	0.71

The reduction in the period of existence of the spring thermal bar, accompanied by a decrease in the area of the northern thermal-inert region of the lake on a fixed date of the annual cycle, is also evidenced by Figure 7, which shows the average positions of the thermal bar (4 °C isolines) on the lake surface over decades (1981–1990, 1991–2000, 2001–2010, 2011–2020), calculated using modeling data for May 15, May 31 and June 15. As seen, the area of the thermal-inert region increases slightly in the period from 1981–1990 to 1991–2000, and then decreases sharply, including the last decade 2011–2020, which is especially clearly seen in Figures 7c and 7d, related to May 31. According to the ISHM, the northern thermal-inert region and, therefore, the thermal bar by this date in the last of the considered decades, 2011–2020, completely disappear.

Estimates of the interannual variability of the mean seasonal ice area of Lake Ladoga for the period 1980–2020 (Figure 8 and Tables 7 and 8) obtained from the SPBEM and ISHM agree with each other better than with the observational data, especially during warm winters, when both models overestimate the mean ice area (Figure 8a). However, on average for the period 1980–2020, SPBEM and ISHM overestimate the ice area by only about 15 and 14%, respectively (Table 7). During the period the ice area decreased by an average of 85 and 68 km^2 per year, respectively, according to SPBEM and ISHM estimates, while the observational data [*Current state...*, 2021] give this decrease of 108 km^2 per year. The duration of the ice existence period decreased from 186, 197 and 194 days in 1980 to 162, 151, 127 days in 2020, i.e. by 24, 46, 67 days, respectively, according to SPBEM, ISHM and observational data (Figures 8b, 8c, Table 8). Note that the estimates of the trends in the average seasonal ice area are significant for both the model data and the observational data (Table 7), which cannot be said about the duration of ice existence: the numbers of days of the onset of ice formation (and, therefore, the duration of ice existence) turned out to be insignificant for the model data and uncorrelated with the observational data (Table 8).

Table 7. Statistical characteristics of the ice area series shown in Figure 8a: $\overline{S}$ – ice area, km^2; D – variance, km^4; b – trend coefficient, $km^2 \cdot year^{-1}$; R^2 – coefficient of determination; p_{level} – significance level; R – correlation coefficient of observational and model data

Parameter	Data source		
	SPBEM	ISHM	OBS
$\overline{S}$	8956	8876	7816
D	5,098,661	3,292,974	11,460,290
b	−85	−68	−108
R^2	0.2	0.2	0.15
p_{level}	0.003	0.003	0.01
R	0.82	0.89	–

Table 8. Statistical characteristics of the series of day snumbers of the onset of ice formation and the disappearance of seasonal ice cover, shown in Figure 8b and 8c: $\overline{N_{day}}$ — average day number; D — variance; b – trend coefficient, $year^{-1}$; R^2 — coefficient of determination; p_{level} — significance level; R — correlation coefficient of observational and model data

Parameter	Figure 8b			Figure 8c		
	Data source					
	SPBEM	*ISHM*	*OBS*	*SPBEM*	*ISHM*	*OBS*
$\overline{N_{day}}$	314	323	333	122	133	128
D	183	150	571	42	236	162
b	0.35	0.27	1.03	−0.25	−0.86	−0.64
R^2	0.09	0.07	0.27	0.21	0.45	0.36
p_{level}	0.05	0.09	0.001	0.003	1.3×10^{-6}	3.0×10^{-5}
R	0.09	0.07	–	0.85	0.69	–

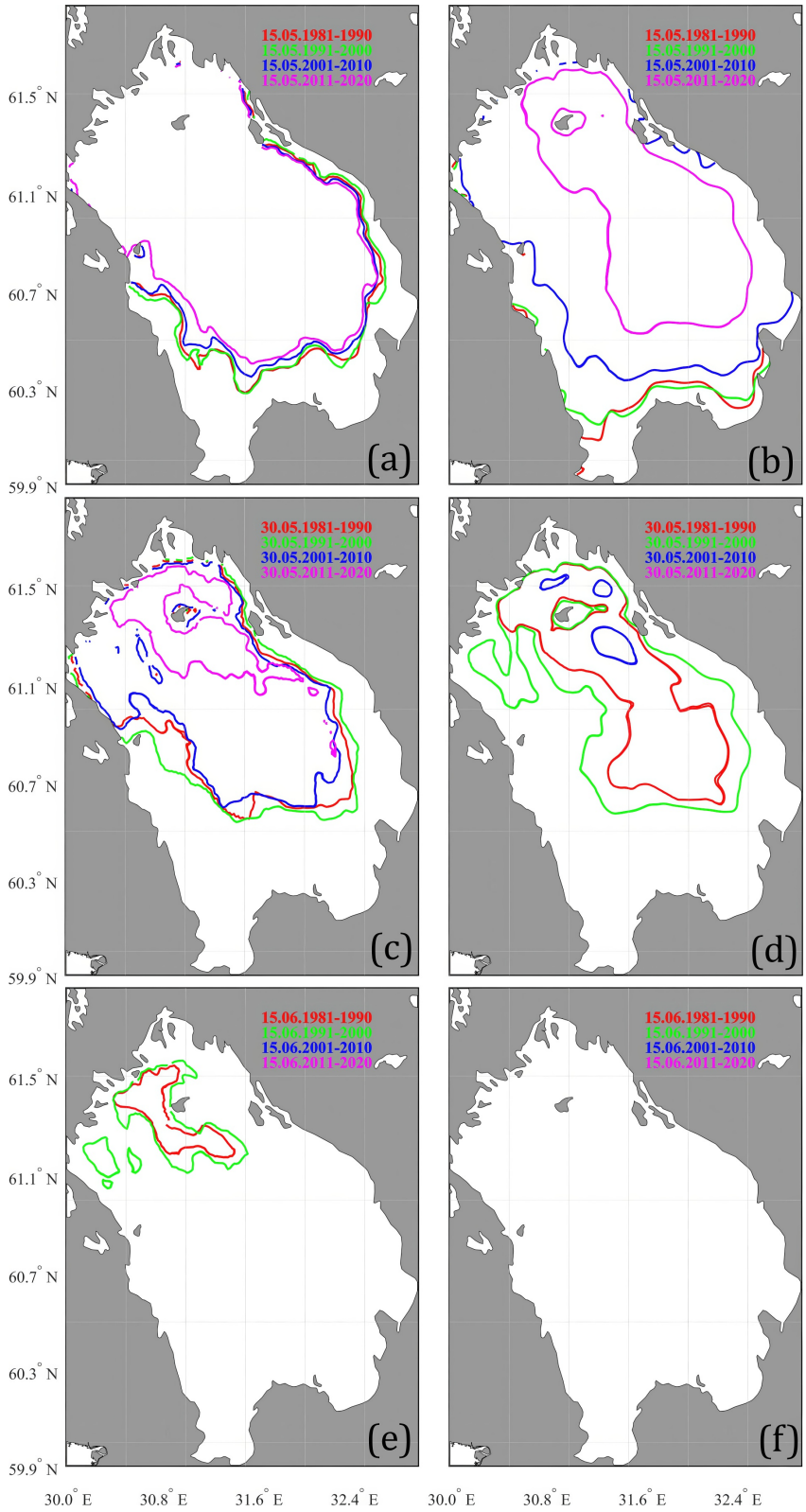

Figure 7. Average decadal positions of the thermal bar (4 °C temperature isolines) based on SPBEM (a, c, e: left column) and ISHM (b, d, f: right column) data for the period 1980–2020. Fragments a, b refer to May 15; fragments c, d – on May 31; fragments d, e – on June15. Isotherms and averaging periods are marked by color: red isolines – 1981–1990; green – 1991–2000; blue – 2001–2010; purple – 2011–2020.

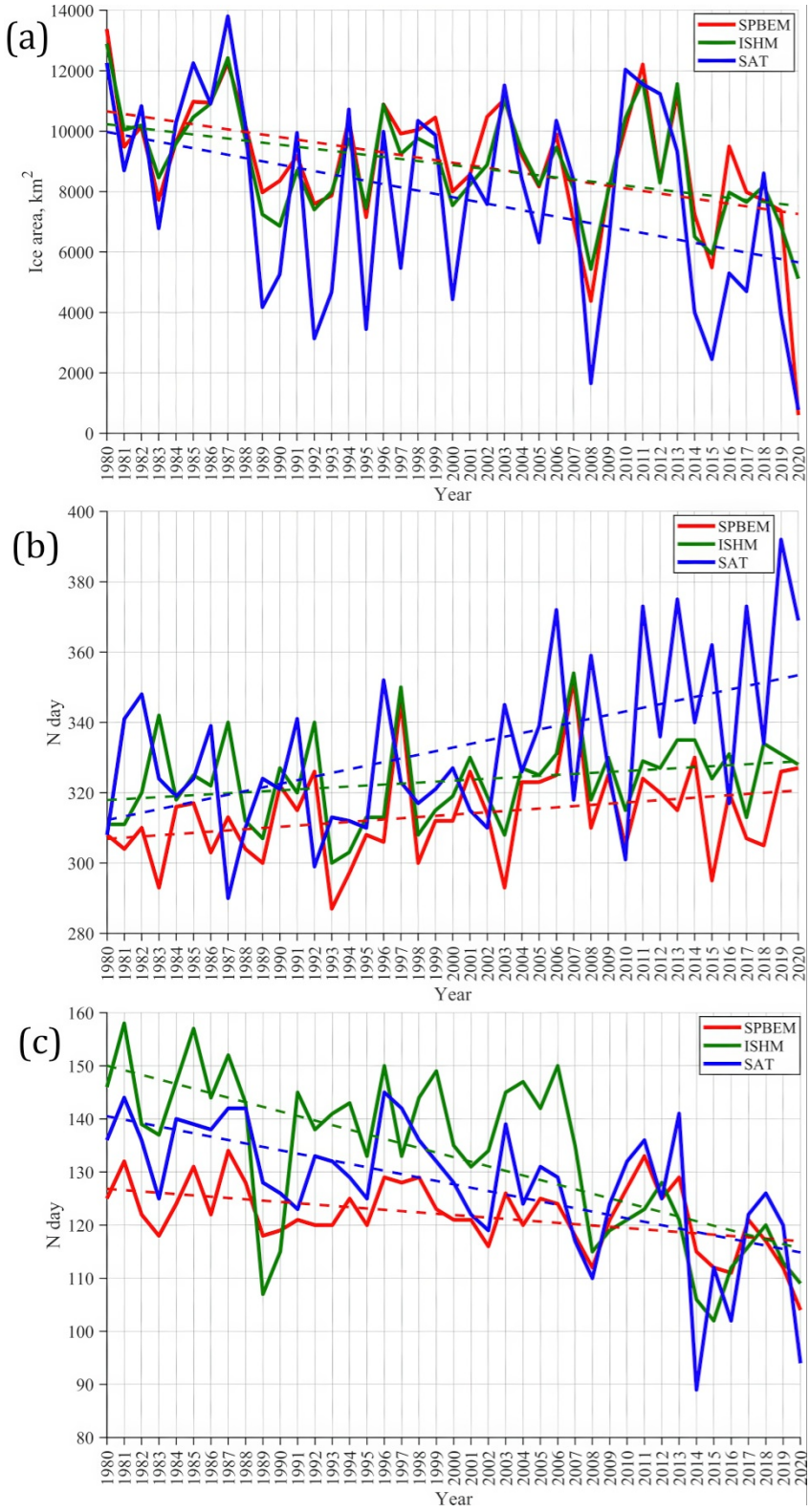

Figure 8. Estimates of the interannual variability of the average seasonal ice area of Lake Ladoga based on aerial photography and satellite measurements (blue curves, OBS) [*Current state...*, 2021], the SPBEM (red curves) and ISHM (green curves) data: a – average ice area for the period of ice existence; b – number of the day of the onset of ice formation; c – number of the day of the disappearance of seasonal ice cover. Linear trends of the characteristics are shown by dashed lines.

4. Summary and Conclusions

The results of reproducing the thermal state of Lake Ladoga in the period 1980–2020 using two models, the St. Petersburg Baltic Eutrophication Model (SPBEM) developed at the St. Petersburg branch of the P. P. Shirshov Institute of Oceanology of RAS, and the Inland Sea Hydrodynamics Model (ISHM) developed at the Marchuk Institute of Computational Mathematics of the RAS and adapted to lake conditions at the Institute of Limnology of the RAS, are compared with data from contact and satellite measurements, as well as with each other. We showed that, in general, both models adequately reproduce the main features of the average state and intra-annual variability of Lake Ladoga. At the same time, both models slightly underestimate the surface temperature of the lake, especially in the summer, compared to satellite monitoring data, that may be a consequence of the features of remote sensing, which measures the temperature of the water surface itself, while model estimates provide the temperature of the upper computational cell with a thickness of 2 m. Assessing the quality of these two models in relation to reproducing the average surface temperature of Lake Ladoga, we note that although SPBEM underestimates the temperature (estimated from satellite data) slightly more than ISHM, it generally reproduces the standard deviation of this characteristic better and correlates better with satellite data, especially during the period of ice cover. The SPBEM model also reproduces the vertical thermal structure of the lake better in the summer. Insufficient accuracy of reproducing the vertical structure by the ISHM model may be associated with the parameterization of vertical mixing poorly adapted to lake conditions.

We showed that it is impossible to obtain significant characteristics of the interannual variability of the surface temperature of Lake Ladoga based on the available satellite data. According to model calculations, the average surface temperature of Lake Ladoga fluctuated in the period 1980–2020, and its average annual value increased by 1.2 (1.7)°C from 5.4 (5.6)°C in 1980 to 6.6 (7.3)°C in 2020, respectively, in SPBEM and ISHM. The temperature increase was greater in the summer period, when it amounted to 1.6 (2.6)°C, and less in the winter period – 0.8 (1.0)°C. At the same time, the average annual temperature of the entire lake (from the surface to the bottom) changed less than the surface temperature: from 4.1 (4.5)°C in 1980 to 4.6 (5.3) in 2020, respectively, in SPBEM and ISHM, i.e. by only 0.5 (0.8)°C.

Estimates of the interannual variability of the average seasonal ice area of Lake Ladoga in the period 1980–2020 according to the SPBEM and ISHM models agree with each other better than with observational data, especially in warm winters, when both models overestimate the average seasonal ice area. However, on average for this period, SPBEM and ISHM overestimate the ice area by only about 15 and 14%, respectively. The ice area has been decreasing by an average of 85 and 68 km^2 per year, respectively, according to SPBEM and ISHM estimates, while observational data shows that this decrease is 108 km^2 per year.

Thus, both presented models reproduce the main features of interannual and intra-annual variability of Lake Ladoga quite well and can be used to reproduce and analyze possible future changes in the lake ecosystem under conditions of changing climate and anthropogenic impacts.

Acknowledgments. The research was supported by grants from the Russian Science Foundation (project No. 23-17-20010) and the St. Petersburg Science Foundation (project No. 23-17-20010).

References

Bennington V., McKinley G. A., Kimura N., et al. General circulation of Lake Superior: Mean, variability, and trends from 1979 to 2006 // Journal of Geophysical Research: Oceans. — 2010. — Vol. 115, no. C12. — https://doi.org/10.1029/2010jc006261.

Chen Ch.-T. A. and Millero F. J. Precise thermodynamic properties for natural waters covering only the limnological range // Limnology and Oceanography. — 1986. — Vol. 31, no. 3. — P. 657–662. — https://doi.org/10.4319/lo.1986.31.3.0657.

Current state and problems of anthropogenic transformation of the ecosystem of lake Ladoga in a changing climate / ed. by S. A. Kondrat'ev, Sh. R. Pozdnjakov and V. A. Rumjancev. — Moscow : RAS, 2021. — 640 p. — (In Russian).

Gaspar P., Grégoris Y. and Lefevre J.-M. A simple eddy kinetic energy model for simulations of the oceanic vertical mixing: Tests at station Papa and long-term upper ocean study site // Journal of Geophysical Research: Oceans. — 1990. — Vol. 95, no. C9. — P. 16179–16193. — https://doi.org/10.1029/jc095ic09p16179.

Golosov S. D., Zverev I. S. and Shipunova E. A. Modeling of thermohydrodynamic processes and ecosystems of Lake Ladoga and Lake Onega based on a 3D model of the hydrodynamics of the inland sea // Diagnosis and forecast of thermohydrodynamics and ecosystems of the Great Lakes of Russia. — Petrozavodsk : KarNC RAS, 2020. — P. 166–197. — (In Russian).

Groisman P., Shugart H., Kicklighter D., et al. Northern Eurasia Future Initiative (NEFI): facing the challenges and pathways of global change in the twenty-first century // Progress in Earth and Planetary Science. — 2017. — Vol. 4, no. 1. — https://doi.org/10.1186/s40645-017-0154-5.

Hersbach H., Bell B., Berrisford P., et al. ERA5 hourly data on single levels from 1940 to present. — 2023. — https://doi.org/10.24381/cds.adbb2d47.

Hibler W. D. Modeling a Variable Thickness Sea Ice Cover // Monthly Weather Review. — 1980. — Vol. 108, no. 12. — P. 1943–1973. — https://doi.org/10.1175/1520-0493(1980)108<1943:mavtsi>2.0.co;2.

Ibrayev R. A. Model of enclosed and semi-enclosed sea hydrodynamics // Russian Journal of Numerical Analysis and Mathematical Modelling. — 2001. — Vol. 16, no. 4. — P. 291–304. — https://doi.org/10.1515/rnam-2001-0404.

Ibrayev R. A. Mathematical modeling of thermohydrodynamic processes in the Caspian Sea. — Moscow : GEOS, 2008. — 127 p. — (In Russian).

Ibrayev R. A. and Trukhchev D. I. Model studies of the seasonal variability of the Black Sea circulation // NATO TU-Black Sea Project: Ecosystem Modelling as a Management Tool for the Black Sea. Vol. 2. — Netherlands : Kluwer Academic Publishers, 1998. — P. 179–196.

Isaev A., Vladimirova O., Eremina T., et al. Accounting for Dissolved Organic Nutrients in an SPBEM-2 Model: Validation and Verification // Water. — 2020. — Vol. 12, no. 5. — P. 1307. — https://doi.org/10.3390/w12051307.

Isaev A. V., Ryabchenko V. A. and Konik A. A. Reproduction of the Current Climatic State of the Lake Ladoga Ecosystem // Fundamental and Applied Hydrophysics. — 2024. — Vol. 17, no. 2. — P. 50–65. — https://doi.org/10.59887/2073-6673.2024.17(2)-5.

Isaev A. V. and Savchuk O. P. Diagnosis of the state of the ecosystem of Lake Ladoga and forecast of changes in case of possible climate change based on mathematical modeling of biogeochemical fluxes of matter // Diagnosis and forecast of thermohydrodynamics and ecosystems of the Great Lakes of Russia. — Petrozavodsk : KarNC RAS, 2020. — P. 197–208. — (In Russian).

Klinger B. A., Marshall J. and Send U. Representation of convective plumes by vertical adjustment // Journal of Geophysical Research: Oceans. — 1996. — Vol. 101, no. C8. — P. 18175–18182. — https://doi.org/10.1029/96jc00861.

Ladoga and Onego - Great European Lakes: Observations and modeling / ed. by L. Rukhovets and N. Filatov. — Berlin Heidelberg : Springer, 2010. — P. 308. — https://doi.org/10.1007/978-3-540-68145-8.

Large W. G. and Pond S. Open Ocean Momentum Flux Measurements in Moderate to Strong Winds // Journal of Physical Oceanography. — 1981. — Vol. 11, no. 3. — P. 324–336. — https://doi.org/10.1175/1520-0485(1981)011<0324:oomfmi>2.0.co;2.

Launiainen J. and Vihma T. Derivation of turbulent surface fluxes - An iterative flux-profile method allowing arbitrary observing heights // Environmental Software. — 1990. — Vol. 5, no. 3. — P. 113–124. — https://doi.org/10.1016/0266-9838(90)90021-w.

Marshall J., Adcrof A., Hill C., et al. A finite-volume, incompressible Navier Stokes model for studies of the ocean on parallel computers // Journal of Geophysical Research: Oceans. — 1997. — Vol. 102, no. C3. — P. 5753–5766. — https://doi.org/10.1029/96jc02775.

Ménesguen A. and Lacroix G. Modelling the marine eutrophication: A review // Science of The Total Environment. — 2018. — Vol. 636. — P. 339–354. — https://doi.org/10.1016/j.scitotenv.2018.04.183.

Menshutkin V. V., Astrakhantsev G. P., Yegorova N. B., et al. Mathematical modeling of the evolution and current conditions of the Ladoga Lake ecosystem // Ecological Modelling. — 1998. — Vol. 107, no. 1. — P. 1–24. — https://doi.org/10.1016/s0304-3800(97)00184-1.

Mooij W. M., Trolle D., Jeppesen E., et al. Challenges and opportunities for integrating lake ecosystem modelling approaches // Aquatic Ecology. — 2010. — Vol. 44, no. 3. — P. 633–667. — https://doi.org/10.1007/s10452-010-9339-3.

Munk W. H. and Anderson E. R. Note on theory of the thermocline // Journal of Marine Research. — 1948. — Vol. 7, no. 3. — P. 276–295.

NASA. Ocean Color Web. — URL: https://oceancolor.gsfc.nasa.gov (visited on 12/12/2024).

Naumenko M. A. and Guzivaty V. V. Climatic variations of the temperature regime of Lake Ladoga for the open water period // Regional'naya ekologiya. — 2010. — Vol. 29, no. 3. — P. 104–108. — (In Russian).

Pilcher D. J., McKinley G. A., Bootsma H. A., et al. Physical and biogeochemical mechanisms of internal carbon cycling in Lake Michigan // Journal of Geophysical Research: Oceans. — 2015. — Vol. 120, no. 3. — P. 2112–2128. — https://doi.org/10.1002/2014jc010594.

Rukhovets L. A., Astrakhantsev G. P., Menshutkin V. V., et al. Development of Lake Ladoga ecosystem models: modeling of the phytoplankton succession in the eutrophication process. I // Ecological Modelling. — 2003. — Vol. 165, no. 1. — P. 49–77. — https://doi.org/10.1016/s0304-3800(03)00061-9.

Ryabchenko V. A., Karlin L. N., Isaev A. V., et al. Model estimates of the eutrophication of the Baltic Sea in the contemporary and future climate // Oceanology. — 2016. — Vol. 56, no. 1. — P. 36–45. — https://doi.org/10.1134/s0001437016010161.

Smagorinsky J., Manabe S. and Holloway J. I. Numerical results from a nine-level general circulation model of the atmosphere // Monthly Weather Review. — 1965. — Vol. 93, no. 12. — P. 727–768. — https://doi.org/10.1175/1520-0493(1965)093<0727:NRFANL>2.3.CO;2.

TEOS-10. Thermodynamic Equation of Seawater - 2010. — 2010. — URL: https://www.teos-10.org.

Vinçon-Leite B. and Casenave C. Modelling eutrophication in lake ecosystems: A review // Science of The Total Environment. — 2019. — Vol. 651. — P. 2985–3001. — https://doi.org/10.1016/j.scitotenv.2018.09.320.

Zhang J. and Hibler W. D. On an efficient numerical method for modeling sea ice dynamics // Journal of Geophysical Research: Oceans. — 1997. — Vol. 102, no. C4. — P. 8691–8702. — https://doi.org/10.1029/96JC03744.

Zverev I. S., Zdorovennov R. E., Zdorovennova G. E., et al. Response of a shallow lake to wind load during the open water period (3d numerical experiments) // Proceedings of the Karelian Research Centre of the Russian Academy of Sciences. — 2020. — No. 9. — P. 5–17. — https://doi.org/10.17076/lim1297. — (In Russian).